Narrow-linewidth near-degenerate optical parametric generation achieved with quasi-group-velocity-matching in lithium niobate waveguides

Xiuping Xie, Jie Huang, and M. M. Fejer

Edward L. Ginzton Laboratory, Stanford University, Stanford, California 94305

Received April 5, 2006; accepted May 5, 2006; posted May 10, 2006 (Doc. ID 69685)

We demonstrate narrow-linewidth near-degenerate optical parametric generation in reverse-proton-exchange lithium niobate waveguides with quasi-group-velocity-matching, which is realized by using wavelength-selective directional couplers and tight-radius bends. With appropriate designs for 1.6 ps long pump pulses at 785.1 nm we obtained near-degenerate signal (idler) pulses with a time–bandwidth product as low as 1.1, compared with 10.5 for conventional devices without quasi-group-velocity-matching. This improvement in the temporal property is a result of both a pulse compression effect and a filter effect coming from our scheme of quasi-group-velocity-matching. © 2006 Optical Society of America

OCIS codes: 190.4410, 230.4320, 190.7110.

The temporal properties of the output have long been a limiting factor for applications of optical parametric generation (OPG). We previously demonstrated controllable temporal properties at desired wavelengths with cascaded OPG in lithium niobate waveguides.[1] The control of temporal properties can also be achieved by directly manipulating the effective group velocities of the interacting waves.[1] Group-velocity matching in nonlinear interactions has been frequently studied in recent years. In bulk materials used for $\chi^{(2)}$ nonlinear interactions it has been realized by using different polarizations or by tilting the wave fronts.[2,3] Such approaches are prohibited in reverse-proton-exchange lithium niobate waveguides because only TM modes are guided and the wave fronts in waveguides cannot be tilted. In this Letter we report the application of an alternative approach, quasi-group-velocity-matching[4] (QGVM), for OPG in reverse-proton-exchange lithium niobate waveguides. With 1.6 ps long pump pulses near 785.1 nm we obtained near-degenerate output pulses with a time–bandwidth product as low as 1.1 from a device with QGVM. Compared with a much larger time–bandwidth product of 10.5 for near-degenerate OPG in a device without QGVM, the temporal properties of OPG pulses are significantly improved.

The QGVM scheme shown in Fig. 1 is similar to that used for second-harmonic generation[4] (SHG). The length of each quasi-phase-matching (QPM) grating is $L_g \sim 4.8$ mm, approximately the group-velocity walkoff length between 1.6 ps long pulses at 785 and 1570 nm. The length of each directional coupler is $L_{\mathrm{DC}} \sim 1$ mm, designed to couple the 1570 nm waves into a different waveguide while keeping the 785 nm waves in the old path. The two directional couplers are connected with a straight waveguide (length L_1) and an s bend (length L_2) so that the signal and the idler (with faster group velocities) will propagate through a longer optical path than the pump. To ensure that the pulse envelopes of the pump and signal (idler) efficiently overlap in every section of the QPM gratings the optimal design must satisfy

$$L_2 - L_1 = (n_g^p/n_g^{s,i} - 1)(rL_g + L_1 + 2L_{\mathrm{DC}}). \qquad (1)$$

Here n_g^j ($j=p,s,i$, respectively corresponding to the pump, signal, and idler) is the group index in straight waveguides. Near degeneracy the same QGVM design works for both the signal and the idler because $n_g^s \approx n_g^i$ and the typical bandwidth of the directional couplers is >100 nm. The ratio r is a noncritical adjustable parameter with an optimal value slightly greater than 1, since the group index in the s bends is slightly smaller than that in straight waveguides.

To have more QGVM sections within a limited device length, we prefer a shorter L_1; the approximate length is proportional to the minimum bend radius R in the s bends. To avoid bend loss, the smallest R is 4 mm in typical reverse-proton-exchange waveguides fabricated with our conventional process,[5] for which the proton-exchange depth is 1.84 μm, the annealing time is 23 h at 310°C, and the time of reverse-proton-exchange is 25 h at 300.5°C. We are able to reduce R to 1 mm without introducing extra bend loss by using a new process in which the proton-exchange depth is increased to 2.39 μm. The price is

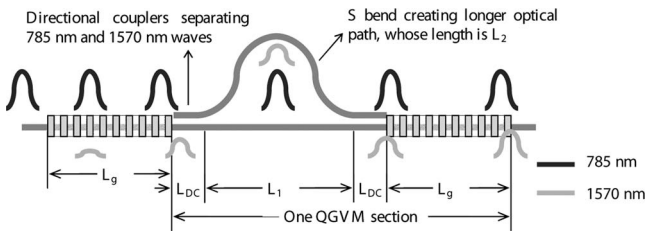

Fig. 1. Near-degenerate OPG using waveguides with one QGVM section, designed for a pump wave near 785 nm and signal and idler waves near 1570 nm. L_g is the length of each section of QPM gratings, L_{DC} is the length of each directional coupler, and L_1 is the length of the straight waveguide between the two directional couplers.

0146-9592/06/142190-3/$15.00

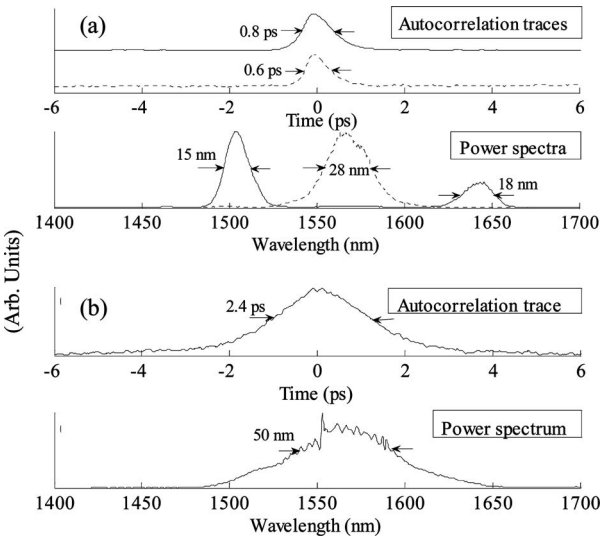

Fig. 2. (a) Autocorrelation traces and power spectra of the output from a device with four QGVM sections; (b) those from a conventional device without QGVM. Solid curves, device temperature of 130°C; dotted curves, 121.3°C. The pump wavelength was 785.1 nm for all. The total length of QPM gratings was 24 mm in both cases. The pulse lengths and bandwidths in the figures are FWHM widths.

a higher propagation loss, <0.25 dB/cm for waves near 1570 nm (compared with that of <0.1 dB/cm with the previous process) and <0.5 dB/cm for waves near 785 nm. For $L_g \sim 4.8$ mm, $L_{DC} \sim 1$ mm, $r=1$, and group indices estimated from SHG measurements, the typical length L_1 is 13.7 mm with the previous process and 4.5 mm with the new process. With the latter we are able to design devices with four QGVM sections on a 60 mm long chip.

We designed devices with both processes to check the effects of multiple QGVM sections and the propagation losses on the gain and temporal properties of the OPG output. The device structures are similar for the two fabrication recipes. The pump wave near 785 nm in the free-space TEM_{00} mode is converted into an almost pure TM_{00} waveguide mode at the beginning of the devices by a single-mode filter,[1] following which are QPM gratings and QGVM sections as shown in Fig. 1. The waveguide widths (defined as the opening on the SiO_2 mask through which the proton exchange takes place) and the mode filters are optimized. For the old process, the waveguide width is 1.5 μm in the mode filter and 8 μm otherwise. For the new process, the mode filter is a 1.5 μm wide segmented waveguide with a duty cycle of 20%,[6] and the waveguide width is 6.5 μm in the other regions.

If not otherwise specified, the chips were heated to 130°C in the experiments to reduce photorefractive damage. For a 1.6 ps long pump pulse near 785 nm the OPG threshold of the devices with four QGVM sections was 100 pJ. This is half the threshold of 200 pJ in a conventional device with a continuous 25 mm long QPM grating[1] and is a consequence of the more effective interaction of the pump and signal (idler) pulses in the QGVM structure.

At a pump power level near the OPG threshold, when pump depletion was negligible, we measured the autocorrelation traces of the signal (idler) pulses by using two-photon absorption in a Si photodiode[7] and recorded the power spectrum with an optical spectrum analyzer. The pump wavelength was 785.1 nm, and the signal and the idler were near degeneracy. The solid curves in Fig. 2(a) show the results from a device with four QGVM sections heated to 130°C. The bandwidth of the signal (idler) near 1503 (1645) nm was 15 (18) nm; the pulse length was 0.56 ps, assuming a Gaussian pulse shape; and the time–bandwidth products were 1.1 for both the signal and the idler. The dotted curves show the output from the same device heated to 121.3°C with the signal and idler merged at 1570 nm. The pulse length was 0.44 ps, the bandwidth was 28 nm, and the time–bandwidth product was 1.5. As a comparison, Figure 2(b) shows the results from a conventional device without QGVM: the bandwidth was >50 nm, the pulse length was 1.7 ps, and the time–bandwidth product was 10.5. The total QPM grating lengths in both cases were 24 mm. The OPG output from a device with four QGVM sections thus is much closer to the transform limit than that from a conventional device.

In the experiments we varied the device temperature T and the pump wavelength λ_p, establishing that for the same device with QGVM the pulse length was a weak function of T and λ_p, while the bandwidth was a strong function of them. Figure 3 shows the power spectra for a device with the simplest QGVM design, which had only one QGVM section and was fabricated with the old process. T was fixed at 130°C for curves in Fig. 3(a). λ_p was fixed at 781.2 nm for curves in Fig. 3(b), and their baselines indicate the various device temperatures, which can be read from the vertical axis. Because of a filter effect coming from the carrier phase mismatch generated in the QPM section the power spectrum changed significantly when λ_p varied by 0.3 nm or T varied by 2°C. This filter effect notably contributed to the im-

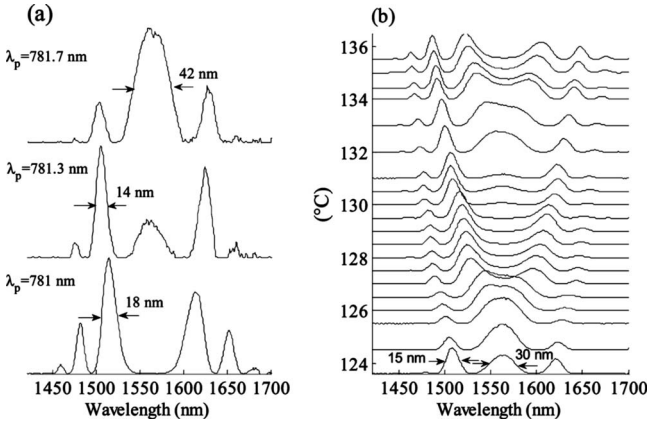

Fig. 3. Power spectra of the output from a waveguide with one QGVM section. The total length of QPM gratings was 9.6 mm. The device temperature was fixed at 130°C in (a). The pump wavelength was fixed at 781.2 nm in (b). The baselines of the curves in (b) indicate the device temperature, which can be read from the vertical axis. All traces are normalized to their maxima. The bandwidths shown in the figures are FWHM widths.

provement in temporal properties of the OPG output. While the results are consistent with numerical simulations, a more insightful explanation comes from analytical solutions to cw optical parametric amplification (OPA).

For cw OPA we can drop the terms corresponding to the group velocities in Eq. (1) in Ref. 1. Suppose the initial phase mismatch between the three interacting waves is $\phi=\phi(\lambda_{s,i})=2\pi[n(\lambda_p)L_1/\lambda_p - n(\lambda_s)L_2/\lambda_s - n(\lambda_i)L_2/\lambda_i]$, originating from the two different paths in a QGVM section. λ_j $(j=p,s,i)$ is the wavelength and $n(\lambda_j)$ is the average refractive index over the corresponding waveguide length. With negligible pump depletion and a uniform QPM grating in a straight waveguide, the output signal photon flux is

$$\begin{aligned} I_s &= I_{s0}\{\cosh^2 \alpha L_g + [\Delta k/(2\alpha)]^2 \sinh^2 \alpha L_g\} \\ &\quad + I_{i0}(\Gamma/\alpha)^2 \sinh^2 \alpha L_g \\ &\quad + 2(\Gamma/\alpha)\sinh \alpha L_g \sqrt{I_{s0}I_{i0}}\{\cosh \alpha L_g \cos \phi \\ &\quad + [\Delta k/(2\alpha)]\sinh \alpha L_g \sin \phi\}, \end{aligned}$$

$$\alpha = \sqrt{\Gamma^2 - \Delta k^2/4}, \quad \Delta k = k_p - k_s - k_i - 2\pi/\Lambda. \qquad (2)$$

$I_{s0}(I_{i0})$ is the input photon flux of the signal (idler), L_g is the length of the QPM grating, Γ is similar to the parametric gain coefficients defined in Ref. 1, k_j $(j=p,s,i)$ is the wave vector, and Λ is the QPM grating period. For OPA $\Gamma \gg \Delta k/2$, and α is real.

Equation (2) can be simplified to $I_s \approx 4I_{s0} \sinh^2 \Gamma L_g \cos^2(\phi/2)$ in the high-gain regime if $\Delta k \approx 0$ and $I_{s0}=I_{i0}$, which are satisfied in the QPM gratings in our QGVM scheme. Each QGVM section thus is a combination of an amplifier with exponential gain and a frequency filter determined by the carrier phase mismatch. Because the functions $\phi(\lambda_{s,i})$ vary by several π within the >150 nm bandwidth for near-degenerate OPA when $L_g \sim 4.8$ mm, the signal power spectrum has several peaks and valleys, and their positions vary when $\phi(\lambda_{s,i})$ changes with T and λ_p, as shown in Fig. 3.

By comparing the results shown in Figs. 2 and 3, we can deduce the effects of multiple QGVM sections. Side peaks are significant in the spectra in Fig. 3 when the device has only one QGVM section, but are negligible in Fig. 2(b) when the device has four QGVM sections. The reason is that each extra QGVM section is an extra frequency filter, and the main peak is thus selected out. However, the bandwidth of the main peak varied only slightly, possibly because each QGVM section randomly introduced a different phase-mismatch function $\phi(\lambda_{s,i})$, and the overall effect was not optimal. More detailed studies need precise control of the carrier phases in each QGVM section, which may be realized in the future by using electro-optical phase shifters.[8]

We also measured and simulated different devices to explore the consequences of the propagation losses. The propagation loss of the pump did not affect the frequency response but reduced the parametric gain in the QPM gratings near the end of the devices and prevented us from obtaining an even lower OPG threshold. The propagation loss of the signal and idler only reduced the photon conversion efficiency.

In summary, with quasi-group-velocity-matching (QGVM) in reverse-proton-exchange lithium niobate waveguides we demonstrated a lower optical parametric generation (OPG) threshold of 100 pJ and a time–bandwidth product as low as 1.1 for outputs near degeneracy. QGVM is therefore an effective approach to improving the temporal properties of the OPG output and may enable more applications based on OPG.

This research was supported by the U.S. Air Force Office of Scientific Research through contracts F49620-02-1-0240 and the Multidisciplinary University Research Initiative (MURI) Center for Photonic Quantum Information Systems (U.S. Army Research Office/Advanced Research and Development Activity program DAAD19-03-1-0199). We acknowledge the support of Crystal Technology, Inc. Xiuping Xie's e-mail address is xpxie@stanford.edu.

References

1. X. Xie, A. M. Schober, C. Langrock, R. V. Roussev, J. R. Kurz, and M. M. Fejer, J. Opt. Soc. Am. B **21**, 1397 (2004).
2. P. Di Trapani, A. Andreoni, C. Solcia, P. Foggi, R. Danielius, A. Dubietis, and A. Piskarskas, J. Opt. Soc. Am. B **12**, 2237 (1995).
3. A. V. Smith, Opt. Lett. **26**, 719 (2001).
4. J. Huang, J. R. Kurz, C. Langrock, A. M. Schober, and M. M. Fejer, Opt. Lett. **29**, 2482 (2004).
5. R. Roussev, X. P. Xie, K. R. Parameswaran, M. M. Fejer, and J. Tian, in *2003 IEEE LEOS Annual Meeting Conference* (IEEE, 2003), Vol. 1, pp. 338–339.
6. M. H. Chou, M. A. Arbore, and M. M. Fejer, Opt. Lett. **21**, 794 (1996).
7. L. P. Barry, P. G. Bollond, J. M. Dudley, J. D. Harvey, and R. Leonhardt, Electron. Lett. **32**, 1922 (1996).
8. D. Marcuse, IEEE J. Quantum Electron. **18**, 393 (1982).